Monolayer-induced band bending in the near-surface region of Ge(111)

A. J. Mäkinen* and G. P. Kushto
Naval Research Laboratory, Washington, DC 20375, USA
(Received 27 February 2011; revised manuscript received 26 April 2011; published 27 June 2011)

Directly grafted organic monolayers on Ge surfaces offer an interesting opportunity to explore aspects of surface passivation and control of electrical properties, namely, *molecular gating*, of semiconductor surfaces. We report our study of the interfacial electronic structures of *n*-type, intrinsic, and *p*-type Ge(111) surfaces that have been chemically modified with various organic monolayers. The monolayers investigated include octadecane, attached via hydrogermylation of 1-octadecene at Ge surfaces, as well as para-substituted phenyl rings, attached by diazonium activation of hydrogenated Ge surfaces. X-ray photoelectron spectroscopy measurements indicate that there is downward band bending, up to 160 meV, associated with assembling these organic monolayers on the Ge substrates. This band bending does not directly correlate with the dipole moment or electron withdrawing or donating character of the molecular moieties, pointing to the critical roles of the nature and quality of the self-assembled monolayer, and the intrinsic electronic structure of the semiconductor material in defining the interfacial electronic structure of the passivated Ge(111) surfaces.

DOI: 10.1103/PhysRevB.83.245315 PACS number(s): 73.30.+y

I. INTRODUCTION

Germanium (Ge) is an attractive high-mobility channel material for replacing Si channels in next generation complementary metal oxide semiconductor (CMOS) devices. However, it is recognized that serious technical challenges need to be overcome before Ge channels can be implemented in CMOS structures. These include (1) high thermal activation of Ge dopants compared with Si and III–V processes and (2) the growth of high-κ dielectrics with *unpinned* Fermi level in the channel material.[1] Therefore, the passivation of Ge surfaces and the control of electrical properties of Ge surfaces and near-surface regions is one of the most important issues for obtaining high-performance CMOS devices with a Ge channel.

Grafting self-assembled monolayers (SAMs) of organic molecules onto a semiconductor surface offers an interesting opportunity to explore aspects of surface passivation and the control of the electrical properties, namely, *molecular gating*, of semiconductor surfaces. While Si surfaces, terminated with alkyl and functionalized aryl groups, have attracted both experimental[2–7] and theoretical[8,9] efforts for quite some time; it is only recently that SAM-terminated Ge surfaces have started to receive a similar level of attention.[10–13]

Molecular chemistry has been very successful in developing and explaining attachment strategies for molecular moieties onto semiconductor surfaces which, owing to their covalent nature, can be described within a molecular framework.[7] For instance, [2 + 2] cycloaddition of alkenes at Si(100) and hydrosilylation at hydrogenated Si(111) and Ge(111) surfaces have analogies in organic synthesis.[6,7] However, this molecular chemistry has been less successful in explaining the electronic properties of the SAM—semiconductor interface resulting from molecular attachment, and there remain many questions about the exact mechanisms leading to changes in the semiconductor band structure in near-surface regions.[12,14,15]

Herein, we have investigated the interfacial electronic structures of Ge(111) surfaces resulting from the grafting of organic monolayers directly onto *n*-type, intrinsic, and *p*-type Ge(111) substrates. The monolayers include alkanes and functionalized aryl groups. X-ray photoelectron spectroscopy (XPS) measurements indicate that there is downward band bending associated with assembling various organic monolayers on the semiconductor substrates. This band bending does not correlate with the dipole moment or electron withdrawing or donating nature of the individual molecular moieties, pointing to the critical role of the molecular grafting process and the intrinsic electronic structure of the semiconductor material in defining the interfacial electronic structure of the passivated Ge(111) surfaces. In fact, we find that the observed band bending is strongly dependent on the type and the level of doping of Ge substrates, implying the presence of donor-like surface states near the conduction band minimum (CBM).

II. EXPERIMENT

Ge(111) substrates (University Wafer) with doping densities 5×10^{18} cm^{-3} (p-Ge), 1×10^{15} cm^{-3} (i-Ge), and 1.6×10^{16} cm^{-3} (n-Ge) were first degreased in a sonicated isopropanol bath for 20 min, followed by 20-min sonication in Milli-Q water (18.3 MΩ) to remove the native oxide layer. Hydrogen-terminated Ge(111) surfaces were prepared by etching Ge substrates in a 10% HF solution for 10 min and then reoxidizing in a 10% H_2O_2 solution for 10 min. Following the soak in H_2O_2, the substrates were sonicated in Milli-Q water for 30 s before being returned to the HF bath. This etch/oxidize process was repeated a total of five times with the final step being the HF etch and drying in a N_2 stream. The Ge(111) surfaces were found to be hydrophobic following the HF etching steps.

The organic SAMs were deposited under a N_2 atmosphere using either diazonium activation or organohydrogermylation of hydrogenated Ge(111) surfaces as reported in detail in Refs. 5 and 6. Briefly, bromobenzene (BB) and nitrobenzene (NB) SAMs were grafted by immersing Ge substrates in 5 mM solutions of either 4-bromobenzenediazonium tetrafluoroborate or 4-nitrobenzenediazonium tetrafluoroborate in anhydrous acetonitrile, respectively, for 1 h. Following surface

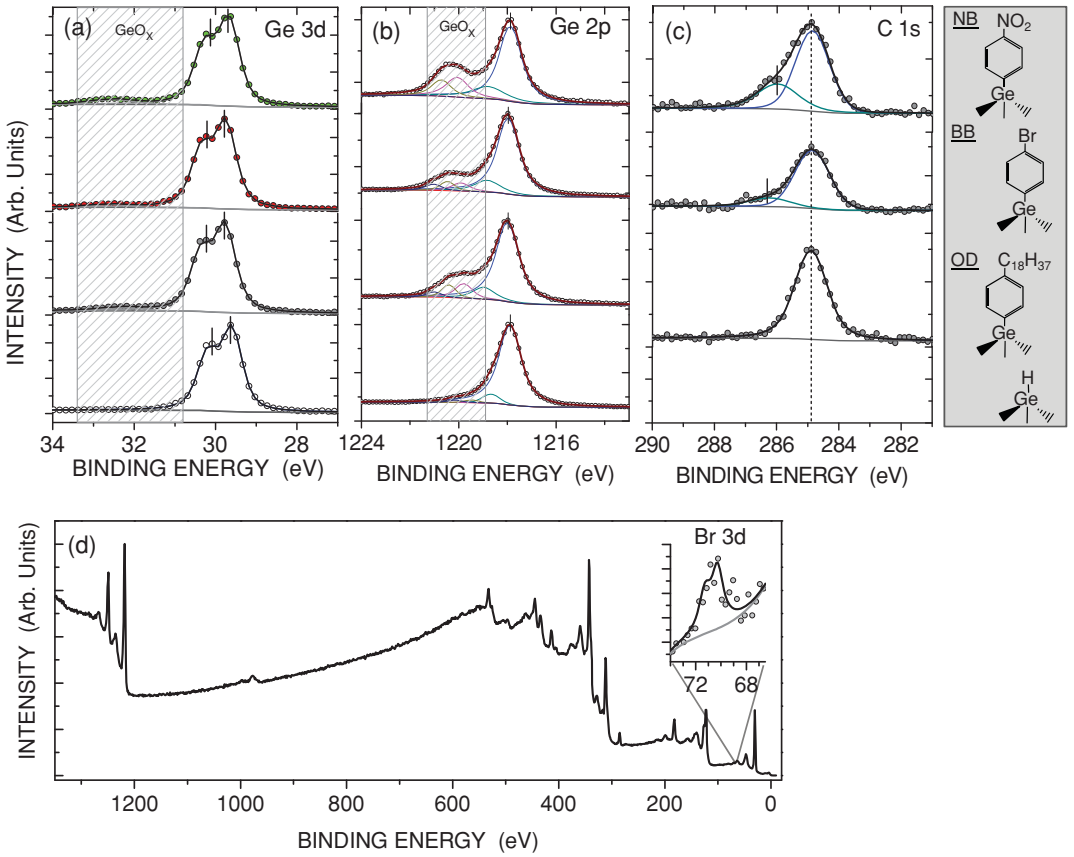

FIG. 1. (Color online) XPS of (a) Ge 3*d*, (b) Ge 2*p*, and (c) C 1*s* core levels for hydrogenated and SAM-covered Ge(111) substrate as indicated in the side bar. The cross-hatched columns indicate the range of binding energies for germanium oxides and suboxides (GeO_x). (d) A survey spectrum of BB SAM-covered Ge(111) substrate.

derivatization, the substrates were rinsed thoroughly with anhydrous acetonitrile to remove excess organic starting material. The 1-octadecane (OD) SAM was prepared by placing Ge substrates in purified 1-octadecene, held at 179 °C, for 2 h. After the octadecane SAM deposition, the Ge substrates were rinsed with hexane, followed by rinse in anhydrous acetonitrile. The Ge substrates were then moved immediately into a vacuum chamber for XPS measurements.

XPS analysis was performed using Thermo Scientific K-Alpha XPS instrumentation with a monochromatic Al Kα source, and the spectral peaks of core levels were fitted using a commercial XPS analysis software by Unifit.

III. RESULTS AND DISCUSSION

The Ge 3*d* core level spectrum for a hydrogenated p-Ge(111) surfaces in Fig. 1 exhibits the well-known doublet feature with a peak separation of 0.6 eV and Ge $3d_{5/2}$ level binding energy (BE) of 29.6 eV. The data were fit to a single Voigt doublet superimposed on a Shirley-type background function. While there were no additional high-BE features in the Ge 3*d* spectrum, the best fit to the more surface-sensitive Ge $2p_{3/2}$ spectrum required high-BE Voigt-singlet peaks, in addition to the elemental $2p_{3/2}$ peak at 1217.9 eV. This suggests the presence of a small amount of surface oxide on the hydrogenated Ge(111) surface.

The carbon 1*s* spectrum of the OD-covered Ge(111) substrate, shown in Fig. 1, is comprised of a single peak at 284.9 eV. In addition to the main peak, also centered at 284.9 eV, the carbon 1*s* spectra of BB- and NB-coated Ge(111) substrates consist of a second peak shifted toward higher BE by 1.4 and 1.1 eV, respectively. The peak separation is consistent with one of the six carbons of the benzene ring bonded to a highly electronegative species.[16,17] The intensity ratio between the high-BE and the main peak for the BB-covered substrate is 0.19 which is very close to the expected value of 0.20 (i.e., 1:5). However, this ratio is 0.3 for the NB-coated substrate, suggesting the presence of more than one carbon atom in a high-BE state per molecule.

After SAM deposition, the Ge 3*d* and 2*p* elemental peaks shift toward higher BE compared to those of the hydrogenated Ge(111) surfaces with the shifts experienced by the 3*d* core lines being larger than those of the 2*p* lines. In addition, the intensity of the oxide peak grows substantially, and is now clearly observed in both the Ge 2*p* and 3*d* spectra. The SAM-induced BE shifts are shown in Fig. 2 as a function of the free-space dipole[8] of the SAM molecule. All the Ge substrates, independent of the substrate doping level, exhibit the same trend in BE shifts: the SAM-induced BE shift is inversely proportional to the free-space dipole of the SAM moiety. In fact, the "slopes" of the quasi-linear plots for BE shifts in Fig. 2 are similar for the different Ge substrates. However, the magnitude of the BE shift, induced by an individual SAM,

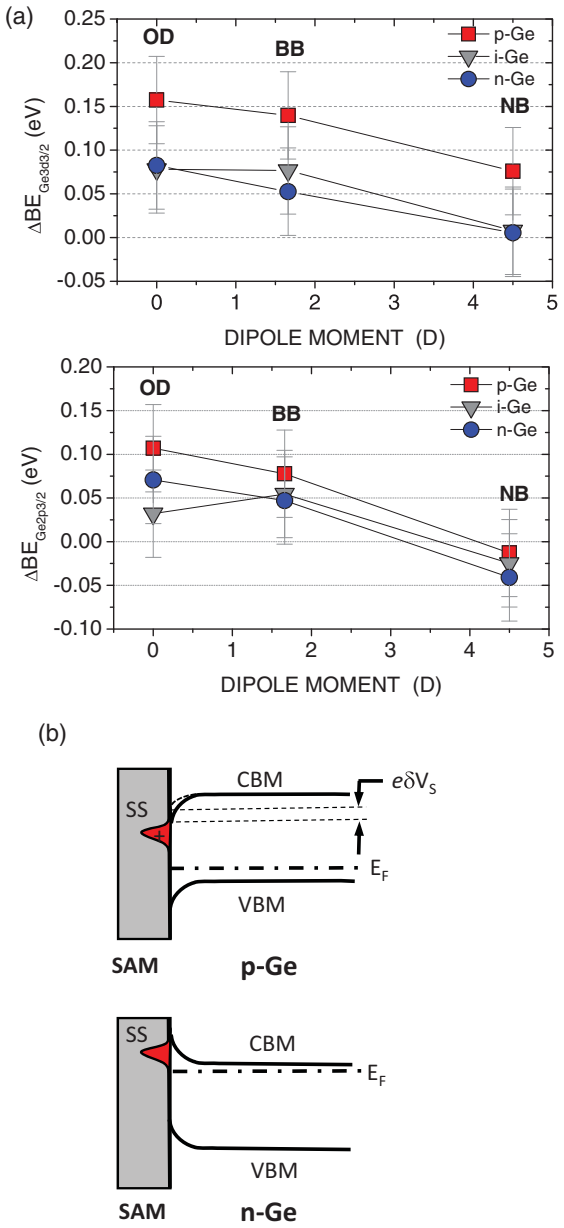

FIG. 2. (Color online) (a) Binding energy shifts of Ge $3d_{3/2}$ and $2p_{3/2}$ core levels for SAM-covered Ge(111) substrates with different doping levels, plotted as a function of the free-space dipole moment of the SAM molecules. (b) Proposed model for the band bending dependence on the substrate doping: donor-like surface states (SS), located near the conduction band minimum (CBM), pin the Fermi level (E_F) in n-Ge(111) substrates, leading to a smaller change in band bending ($e\delta V_s$).

is dependent on the doping of the Ge substrate with the p- and n-doped substrates exhibiting the biggest and smallest BE shifts, respectively.

The shift in the Ge $3d$ and $2p$ core levels toward higher BE can be interpreted as a change in band bending in downward direction, induced by the grafted molecular layers. In the absence of an external field, band bending in semiconductors results from the redistribution of electric charge near a surface or an interface region. Downward band bending (eV_S) implies the presence of additional positive charge at a SAM-covered Ge(111) surface and is proportional to the total amount of the surface charge (Q_{SC}):

$$eV_S = \frac{eQ_{SC}d}{\epsilon\epsilon_0}, \tag{1}$$

where e is the elementary charge, d is the width of the space charge layer, approximated by a step function, and ϵ is the dielectric constant.[18] The doping dependence of the SAM-induced band bending can be understood by attributing the positive surface charge to donor-like surface states residing near the CBM as depicted in Fig. 2. As these surface states are created at the p-Ge(111) surface they are expected to retain their positive charge. However, at the i-Ge(111) and n-Ge(111) surfaces, the surface states reside closer to the Fermi level (located closer to the CBM) and will undergo partial decharging as the Fermi level stabilizes leading to a reduced amount of surface charge and smaller change in downward band bending. In an extreme case, this effect is also known as pinning of the Fermi level.[18] Using Eq. (1) and that $Q_{SC} \approx N_A d$, where N_A is the doping density of p-Ge, we arrive at a surface charge density of $\sim 2.7 \times 10^{12}$ cm^{-2}. Since the atomic density of the Ge(111) surface is 7.2×10^{14} cm^{-2}, the additional positive charge, induced by the SAM fabrication, is $3.8 \times 10^{-3}e$ per Ge atom. Assuming that the density of state associated with the surface states is proportional to the change in surface charge, it is clear that photoemission spectroscopy does not have sufficient sensitivity to observe these surface states directly. Since the current approach is limited in characterizing the surface states further, we can only speculate about the origin of these states, but we want to note that defect-related surface states near the CBM have been observed through scanning tunneling spectroscopy measurements on reconstructed Ge(111)$c(2 \times 8)$ surface.[19]

The limited band bending observed for SAM-covered n-Ge(111) substrates may appear reminiscent of Fermi level pinning (FLP) associated with Schottky barrier formation in *direct* metal/n-Ge contacts. The FLP at metal/n-Ge interface leads to a constant Schottky barrier height, independent of the metal work function.[20,21] Based on these recent experimental findings and earlier theoretical calculations,[22] it has been argued that the strong FLP occurs at the charge neutrality level, near the valence band edge of Ge, and can be characterized by the metal-induced gap states (MIGSs) model. Since MIGSs are absent in the SAM-covered Ge(111) substrates investigated here, we maintain that the SAM-induced band bending effects are distinct of those related to MIGS in direct metal/Ge contacts. In fact, Sharp *et al.*[12] recently found in their *I-V* and *C-V* measurements of alkylated Ge(111) and Ge(100) substrates that a liquid Hg-contact to OD-covered i-Ge substrate exhibited negative flatband potential, i.e., downward band bending, while n-Ge substrates were characterized by a positive flatband potential (0.29 V), implying the absence of MIGS-induced FLP.

The lack of correlation between the free-space dipole moment of the SAM molecules and the induced BE shifts of Ge levels is not necessarily surprising given that the electric field is mostly contained within the dipole layer.[23] A simple charge transfer model proposed in earlier reports for Si surfaces terminated with aryl groups[14,15] does not seem to explain the

differences in the magnitude of band bending, induced by different SAMs. While BB and NB SAMs might be expected to produce the largest band bending effect because of the high electronegativity of the para-substituents of the benzene ring, our core level shifts shown in Fig. 2 indicate the opposite. Therefore, we believe that trends observed for core level shifts in Fig. 2 may be dominated by individual SAM coverage and quality.

The estimate for the SAM thickness can be obtained by calculating the ratio of the measured core level intensities for the SAM (C 1*s*) and the substrate (Ge 2*p* or Ge 3*d*):

$$\frac{I_{\mathrm{C}\,1s}}{I_{\mathrm{Ge}\,3d}} = \frac{\sigma_{\mathrm{C}\,1s} T_{\mathrm{C}\,1s} \lambda^{Q}_{\mathrm{C}\,1s} N_{\mathrm{C}}}{\sigma_{\mathrm{Ge}\,3d} T_{\mathrm{Ge}\,3d} \lambda^{Q}_{\mathrm{Ge}\,3d} N_{\mathrm{Ge}}} \frac{1-\exp\left(-\frac{d}{\lambda^{\mathrm{SAM}}_{\mathrm{C}\,1s}}\right)}{\exp\left(-\frac{d}{\lambda^{\mathrm{SAM}}_{\mathrm{Ge}\,3d}}\right)}, \quad (2)$$

where T is the analyzer transmission function, σ_x is the total photoelectron cross section, N_x is the elemental atomic density, and d is the SAM thickness.[24] The electron attenuation length for quantitative analysis, $\lambda^{Q}_{\mathrm{Ge}\,3d}$, and the practical electron attenuation lengths, $\lambda^{\mathrm{SAM}}_{\mathrm{C}\,1s}$ and $\lambda^{\mathrm{SAM}}_{\mathrm{Ge}\,3d}$, were calculated using NIST Standard Reference Database 82.[25] The calculated value of $\lambda^{Q}_{\mathrm{Ge}\,3d}$, 3.27 nm, compares well with experimentally determined electron escape depths for the corresponding kinetic energies.[26] The lines in Fig. 3(a) depict the intensity ratios calculated from Eq. (2) as a function of the SAM thickness for each of the SAM-covered Ge(111) substrates with the measured intensity ratios indicated by solid data markers. The deduced SAM thicknesses are 1.9–2.0, 1.8–2.1, and 2.4–2.6 nm for OD, BB, and NB SAM, respectively. The OD SAM thicknesses are slightly smaller than those previously reported (2.1–2.5 nm) for octadecane layers prepared on Ge(111) surfaces.[10] The thickness estimates for the BB and NB SAMs appear high, given the shorter van der Waals lengths of the benzene derivatives (0.66 nm for BB and 0.68 nm for NB based on semiempirical molecular orbital calculations) compared with that of the OD molecule. The higher than expected layer thicknesses can be explained by possible multilayer formation, especially in the case of NB SAMs with the highest apparent layer thickness. The presence of multilayers is supported by the intensity ratios of the components of C 1*s* core level spectra shown in Fig. 1. The ratio of 0.3 is significantly higher than the expected 1:5 based on the presumed bonding states of the six carbons in the NB molecule. The increase in the high-BE component of the C 1*s* spectrum can be attributed to a higher number of ring carbons bonded to nitrogen as a result of possible polymerization,[16] leading to higher overlayer thicknesses.

The fraction of the oxide coverage (θ) found on the Ge substrates can be estimated from the intensity ratios of Ge 2*p* and 3*d* levels of the substrate and the oxide:

$$\frac{\left(I^{\mathrm{ox}}_{2p}/I^{B}_{2p}\right)}{\left(I^{\mathrm{ox}}_{3d}/I^{B}_{3d}\right)} = \frac{\left[1-A^{\mathrm{ox}}_{2p}\right]\left[A^{S}_{3d}+\left(A^{\mathrm{ox}}_{3d}-A^{S}_{3d}\right)\theta\right]}{\left[1-A^{\mathrm{ox}}_{3d}\right]\left[A^{S}_{2p}+\left(A^{\mathrm{ox}}_{2p}-A^{S}_{2p}\right)\theta\right]}, \quad (3)$$

where $A^{\mathrm{ox}}_{2p,3d} = \exp(-d^{\mathrm{ox}}/\lambda^{\mathrm{ox}}_{2p,3d})$ and $A^{S}_{2p,3d} = \exp(-d^{S}/\lambda^{S}_{2p,3d})$ are the attenuation factors for the oxide layer and the SAM, respectively, and $\lambda^{\mathrm{ox}}_{2p,3d}$ and $\lambda^{S}_{2p,3d}$ are the practical electron attenuation lengths, calculated as described earlier.[24] The expression (3) was derived following the approach outlined by Tabet and Salim[27] for partially oxidized

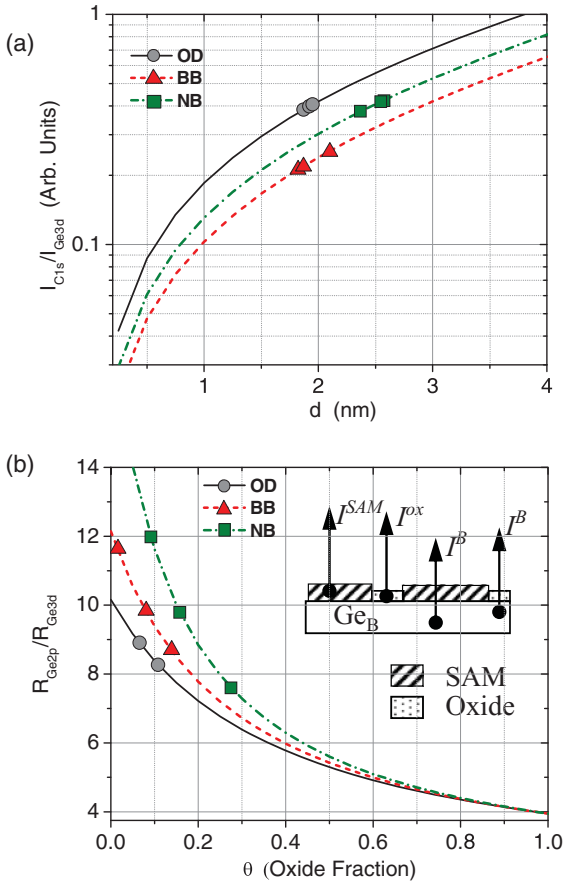

FIG. 3. (Color online) (a) Measured (solid circles) and calculated [solid lines, from Eq. (2)] intensity ratios of the substrate (Ge 3*d*) and overlayer (C 1*s*) signals for SAM-covered Ge(111) substrates, shown as a function of SAM thickness (d). (b) Measured (solid circles) and calculated [solid lines, from Eq. (3)] intensity ratio of the substrate and oxidized Ge 2*p* and 3*d* signals, shown as a function of surface oxide fraction (θ). The inset shows relevant XPS signals from a SAM-covered and partially oxidized Ge(111) substrate.

Ge surfaces. The calculated intensity ratios are plotted as a function of the oxide fraction θ in Fig. 3(b), with the measured intensity ratios indicated by solid data markers. The oxide thickness (d_{ox}) was set at 0.2 nm, in agreement with literature values reported for similarly prepared Ge(111) surfaces,[13,28] and the SAM thicknesses (d_S) were calculated from Eq. (2) as shown in Fig. 3(a). The estimated oxide fractions are similar for OD- and BB-covered substrates: 7%–11% and 2%–14% for the former and latter, respectively. Ge substrates with NB SAM exhibit higher oxide coverage of 9%–28%. For comparison, decyl-terminated Ge(111) surfaces, prepared through organohydrogermylation, have recently been reported to exhibit 30% oxide coverage.[13] The higher oxide fraction of the NB-covered substrates may not be surprising given the evidence for multilayer formation as a result of possible polymerization of NB moieties. It is reasonable to expect the higher degree of substrate oxidation to be associated with poor monolayer formation and compromised passivation of the substrate surface.

With consistent ML layer formation on semiconductor surfaces, molecular gating and passivation can be envisioned

as an enabling technology for electronic applications. For instance, molecular passivation of active structure could be utilized in between different processing steps where other means of protecting the active structure are either not available or are cost prohibitive. Other examples include using SAMs as dopant vehicles, providing a source of dopant atoms for rapid thermal annealing-based surface channel doping.[29]

IV. CONCLUSION

XPS measurements of SAM-covered Ge(111) reveal substrate core level shifts toward higher binding energy, interpreted as a change in downward band banding. This band bending depends on the doping type and level of Ge substrates, leading us to propose the presence of donor-like surface states near the CBM, activated by the molecular grafting process. The electronegativity of the parasubstitute on benzene ring or the dipole moment of the SAM molecule seems to have little or no effect on the magnitude or direction of induced change in band bending. Instead, the changes in the electron band positions are dominated by individual SAM coverage and quality.

ACKNOWLEDGMENTS

The authors would like to thank the Office of Naval Research for support of this work.

*Antti.Makinen@nrl.navy.mil

[1] International Technology Roadmap for Semiconductors, 2010 Update [www.itrs.net].
[2] M. R. Lindford and C. E. D. Chidsey, J. Am. Chem. Soc. **115**, 12631 (1993).
[3] A. Bansal, X. Li, I. Lauermann, and N. S. Lewis, J. Am. Chem. Soc. **118**, 7225 (1996).
[4] H. Haick, P. T. Hurley, A. I. Hochbaum, P. Yang, and N. S. Lewis, J. Am. Chem. Soc. **128**, 8990 (2006).
[5] M. P. Stewart, F. Maya, D. V. Kosynkin, S. M. Dirk, J. J. Stapleton, C. L. McGuiness, D. L. Allara, and J. M. Tour, J. Am. Chem. Soc. **126**, 370 (2003).
[6] J. M. Buriak, Chem. Rev. **102**, 1271 (2002).
[7] S. F. Bent, Surf. Sci. **500**, 879 (2002).
[8] A. Natan, Y. Zidon, Y. Shapira, and L. Kronik, Phys Rev. B **73**, 193310 (2006).
[9] A. Y. Anagaw, R. A. Wolkow, and G. A. DiLabio, J. Phys. Chem. C **112**, 3780 (2008).
[10] J. He, Z.-H. Lu, S. A. Mitchell, and D. D. M. Wayner, J. Am. Chem. Soc. **120**, 2660 (1998).
[11] P. W. Loscutoff and S. Bent, Annu. Rev. Phys. Chem. **57**, 467 (2006).
[12] I. D. Sharp, S. J. Schoell, M. Hoeb, M. S. Brandt, and M. Stutzmann, Appl. Phys. Lett. **92**, 223306 (2008).
[13] D. Knapp, B. S. Brunchwig, and N. S. Lewis, J. Phys. Chem. C **114**, 12300 (2010).
[14] T. He, H. Ding, N. Peor, M. Lu, D. A. Corley, B. Chen, Y. Ofir, Y. Gao, S. Yitzchaik, and J. M. Tour, J. Am. Chem. Soc. **130**, 1699 (2008).
[15] T. He, D. A. Corley, M. Lu, N. Halen, Di Spigna, J. He, D. P. Nackashi, P. D. Franzon, and J. M. Tour, J. Am. Chem. Soc. **131**, 10023 (2009).
[16] K. Roodenko, M. Gensch, J. Rappich, K. Hinrichs, N. Esser, and R. Hunger, J. Phys. Chem. B **111**, 7541 (2007).
[17] A. F. Lee, Z. Chang, S. F. J. Hackett, A. D. Newman, and K. Wilson, J. Phys. Chem. C **111**, 10455 (2007).
[18] H. Luth, *Surfaces and Interfaces of Solid Materials* (Springer, New York, 1997).
[19] R. M. Feenstra, J. Y. Lee, M. H. Kang, G. Meyer, and K. H. Rieder, Phys. Rev. B **73**, 035310 (2006).
[20] A. Dimoulas, P. Tsipas, A. Sotiropoulos, and E. K. Evangelou, Appl. Phys. Lett. **89**, 252110 (2006).
[21] T. Nishimura, K. Kita, and A. Toriumi, Appl. Phys. Lett. **91**, 123123 (2007).
[22] J. Tersoff, Phys. Rev. Lett. **52**, 465 (1984).
[23] V. S. L'vov, R. Naarman, V. Tiberkevich, and Z. Vager, Chem. Phys. Lett. **381**, 650 (2003).
[24] D. Y. Petrovykh, J. C. Smith, T. D. Clark, R. Stine, L. A. Baker, and L. J. Whitman, Langmuir **25**, 12185 (2009).
[25] C. J. Powell and A. Jablonski, *NIST Electron Effective-Attenuation-Length Database*, Version 1.2 (SRD-82) (US Department of Commerce, National Institute of Standards and Technology, Gaithersburg, MD, 2009).
[26] H. Gant and W. Monch, Surf. Sci. **105**, 217 (1981).
[27] N. A. Tabet and M. A. Salim, Appl. Surf. Sci. **134**, 275 (1998).
[28] T. Deegan and G. Hughes, Appl. Surf. Sci. **123/124**, 66 (1998).
[29] J. C. Ho, R. Yerushalmi, Z. A. Jacobson, Z. Fan, R. L. Alley, and A. Javey, Nat. Mater. **7**, 62 (2008).